INSTITUTE OF PHYSICS PUBLISHING NANOTECHNOLOGY
Nanotechnology **17** (2006) 2689–2694 doi:10.1088/0957-4484/17/10/041

Standing [111] gold nanotube to nanorod arrays via template growth

Hong-Wen Wang[1,3], Chain-Fang Shieh[1], His-Yi Chen[1], Wei-Chuan Shiu[1], Bryan Russo[2] and Guozhong Cao[2]

[1] Department of Chemistry, Center for Nanotechnology, Chung-Yuan Christian University, Chungli 320, Taiwan, Republic of China
[2] Department of Materials and Science and Engineering, University of Washington, Seattle, WA 98195, USA

Received 4 January 2006, in final form 28 February 2006
Published 8 May 2006
Online at stacks.iop.org/Nano/17/2689

Abstract
Standing [111]-oriented crystalline gold nanotube (AuNT) and nanorod (AuNR) arrays using electrochemical deposition through template growth are reported. Segments of single crystal and bamboo-like crystalline AuNR arrays with growing direction of [111], having a diameter of 100–150 nm and a length of 10 μm, standing perpendicular to Ti metal foil substrates, are synthesized. The as-synthesized AuNTs and AuNRs are characterized by powder and five circle x-ray diffractometry, UV–visible molecular absorption spectrometry, field emission scanning electron microscopy, and transmission electron microscopy. AuNRs and AuNTs are formed by starting with a tube and the wall of the tube gets progressively thicker and eventually sealed up to form nanorods. Optical absorption at 548 and 578 nm wavelength for gold nanotubes and nanorods, respectively, caused by the transverse (width) mode is identified.

1. Introduction

One-dimensional (1D) metallic nanorods have attracted considerable attention in recent years because of their novel physical properties and potential applications as interconnects in nanometre-scale electronics [1, 2]. The progress in this field has been accelerated by advances in both synthetic methods of preparing the nanoporous templates [2, 3], and development of techniques capable of filling the pores of such membranes [2–7]. Examples of long aspect ratio nanoporous membranes include nanochannel glass membranes, anodized aluminium substrates, and various polymeric membranes. Filling of the pores of such membranes with long aspect ratio nanorods has been accomplished by electro-deposition [2–7], high-pressure metal melt injection [8], and photochemical methods [9]. Metal nanorods (such as Au, Ag, Cu, Ni, Co, etc) with single crystal and polycrystalline structures have been synthesized using the template synthetic method [10–20]. For most reports, random and polycrystalline gold nanorods were present. However, Tian [10, 11] successfully prepared single crystal and polycrystalline metal nanorods (average diameter of 40 nm and a length of 3–5 μm) using 10 nm polycarbonate membrane and the help of gelatin additives. 2D growth was proposed for single crystal gold nanorods and 3D growth for polycrystals [10]. However, for potential and specific applications, standing Au nanorod or nanotube arrays with diameter around 100 nm and length longer than 10 μm might be required. In the present study, crystalline gold nanotubes and nanorods standing and oriented along [111] by electrochemical deposition without gelatin additives is presented. Based on the growth of Au nanotubes and nanorods, the formation mechanism from nanotubes and gradually into nanorods is proposed.

2. Experimental details

1 wt% gold (III) solutions for the electrochemical deposition were prepared by dissolving 1 g gold foils into 10 ml aqua regia solution which was subsequently diluted to 100 ml using de-ionized water. Gentle heating up to 90 °C is required for a rapid and complete dissolution of the gold foils within 30 min. No other organic additives were added. Gold concentrations of 0.05, 0.1, 0.15, and 0.2 wt% were prepared. Gold nanorod arrays were grown inside polycarbonate (PC) templates according to the electrochemical deposition method

[3] Author to whom any correspondence should be addressed.

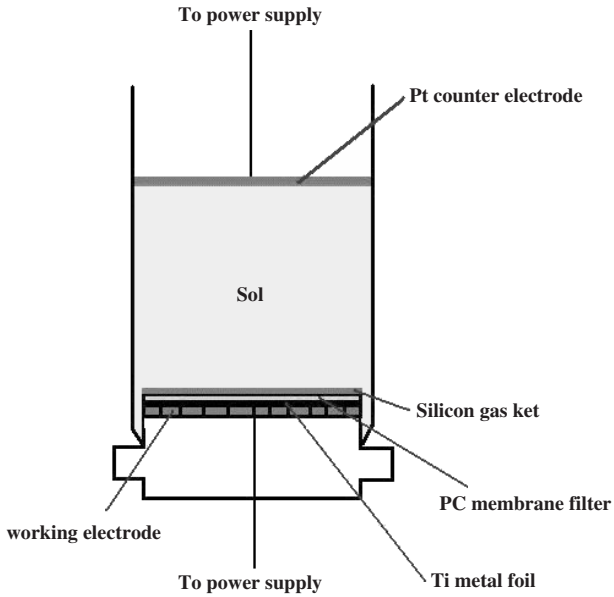

Figure 1. Set-up for electrochemical deposition through template-growth.

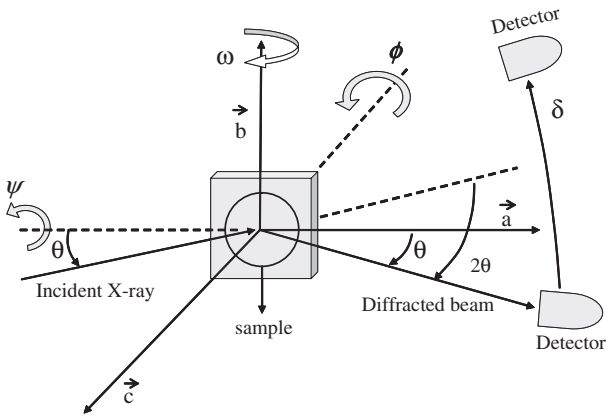

Figure 2. The five circle diffractometer and conventional definition of the angles.

reported in the literature [4, 10]. The templates used were radiation track-etched hydrophilic polycarbonate (PC) membrane (Millipore, Bedford, MA) with pore diameters of 50 and 100 nm and thickness of 10 μm. To ensure a good electric contact, the back of the membrane template was firstly sputter-coated with Au before being attached to the working electrode. An aluminium sheet of 9 mm diameter was used as the working electrode and placed beneath the template, and a Pt mesh was used as a counter-electrode. The distance between the two electrodes was kept at 30 mm. A detailed description of the deposition set-up is shown in figure 1, which was constructed using a syringe. The applied voltage was 0.5, 1.0, 1.5, 2.0, 2.5, 3.0, 4.0, or 5.0 V, and the deposition lasted 0.5–5 h. Upon the completion of deposition, the samples were dried at 90 °C for 12 h in air. Dried samples were subsequently attached onto a piece of titanium plate using silver paste. After drying in an oven at 90 °C overnight, the samples with titanium plate were then immersed in methylene chloride for 30 min to dissolve the PC membrane.

A wide angle powder x-ray diffractometer (WAXRD) and a five circle thin film XRD diffractometer were employed to characterize the crystal structure and crystal orientation of gold nanorods. The WAXRD was performed on a Rigaku D/MAX-3C powder x-ray diffractometer with a Cu target and Ni filter at a scanning rate of 0.1°/1.5 s from $2\theta = 20°$ to 100°. The five circle thin film XRD was carried out using a Rigaku RU-H3R generator together with a Huber diffractometer. The five circle definition is shown in figure 2. Diffraction intensities are collected for three angles, i.e. specimen spin angle (ϕ), rocking angle (ω, i.e. θ at fixed 2θ) and conventional diffracted angle (θ–2θ moves). Two theta is step scanned from 36.1° to 40.1° at a speed of 0.01°/15 s. Rocking angle omega is scanned from 0° to +10° (i.e. $\theta = 19°$–29°) at a speed of 0.01°/30 s while the detector is fixed at $2\theta = 38.1°$ (the main peak [111] position of Au). The ϕ angle (i.e. the sample self-spin angle) is rotated at a speed of 0.5°/30 s from 0 to 360° while the incident x-ray stays in the plane of membrane ($\psi = 90°$) and the detector maintains its position in the plane of the membrane at $\delta = 38.1°$.

The Au nanorods/Au nanotubes (AuNRs/AuNTs) were attached on a piece of glass by tapes and subjected to powder WAXRD experiments without dissolving away the PC membranes (i.e. AuNRs/AuNTs were imbedded in the PC membrane and standing vertically to the glass substrate). XRD experiments were also performed on free-standing AuNRs and aligned AuNRs on Ti metal substrates after dissolving away the PC membranes. A field emission scanning electron microscope (FESEM, JEOL 4100 and Philips JSM 7400) was used to characterize the morphology of nanorod/nanotube arrays. Transmission electron microscopy (TEM) images and electron diffraction patterns were recorded using JEOL 2010 microscopes at accelerating voltage of 200 kV. The gold nanorods or nanotubes were dispersed in 5 ml de-ionized water and collected in a quartz cuvette for the UV–visible test. The absorption spectra were recorded using a Shimadzu UV-1700 ultraviolet–visible photodiode array spectrophotometer.

3. Results and discussion

Figures 3(a)–(c) shows that standing gold nanorods were successfully synthesized on a piece of titanium metal foil using 100 nm membrane templates. Standing gold nanorods were glued on the titanium metal foil by silver paste. These gold nanorods were 100–150 nm in diameter and 10 μm in length. The diameter of each wire was found to be narrower on both ends of the wire. This is caused by the porous membranes used. It appears that the nominal pore diameters quoted by the manufacturer are the values of the pore opening near the surface for filtration purposes. Well aligned gold nanorods standing on the titanium substrate viewed from the top are demonstrated in figure 3(b). These gold nanorods are solid as a close view shows in figure 3(c). However, when the concentration of the gold solution is lower than 0.1 wt% and the deposition voltage is at 1 V, gold nanotubes result, as shown in figure 3(d). The deposition duration for nanotubes is around 2–4 h. Deposition time shorter than 2 h results in incomplete nanotubes. For duration longer than 5 h, nanorods will dominate. These aligned nanotubes or nanorods are

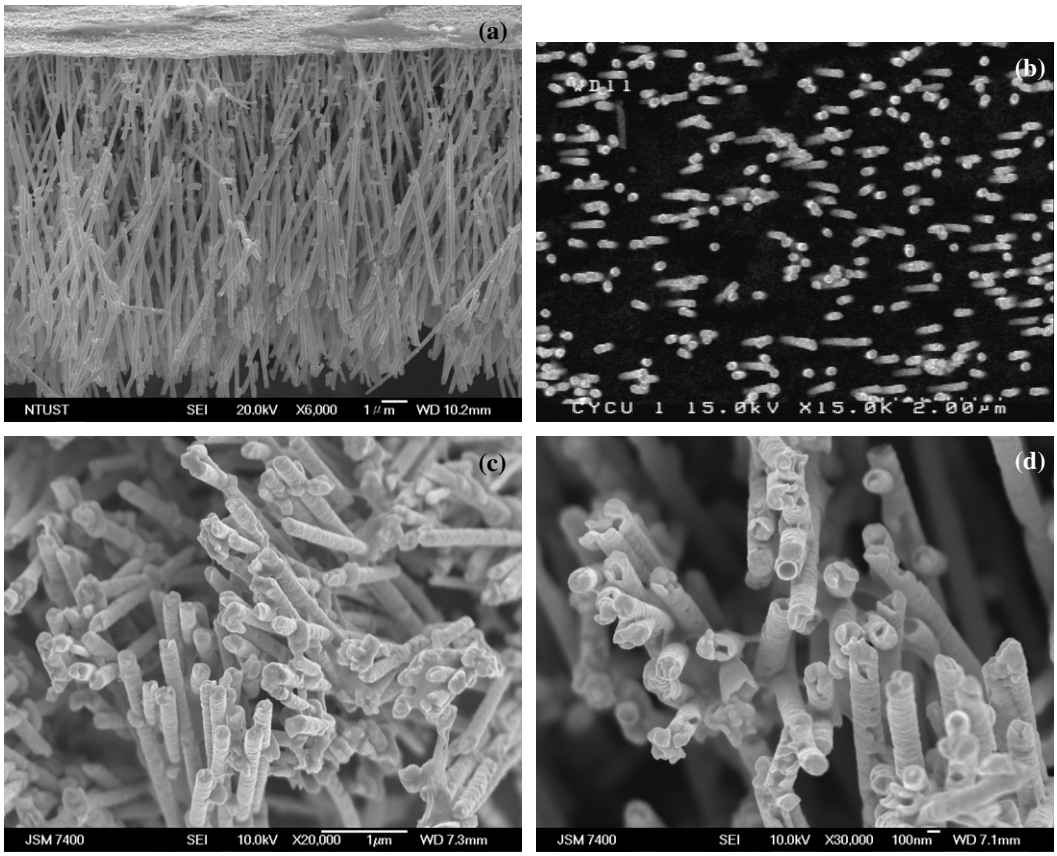

Figure 3. FESEM micrographs for Au nanorod arrays (0.1 wt% conc./1.5 V/3 h): (a) lateral view; (b) top view; (c) top view, large magnification; (d) Au nanotubes (0.1 wt% conc./1.0 V/2 h), top view.

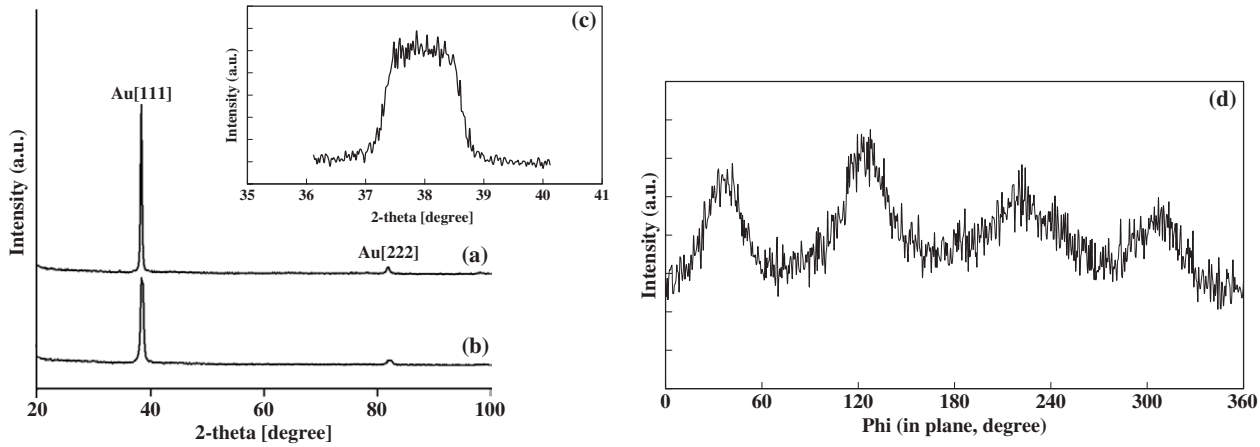

Figure 4. [111] and [222] peaks of (a) Au nanorods and (b) Au nanotubes, θ–2θ analysed by WAXRD; (c) 2θ step scan on [111], and (d) ϕ angle scan with δ angle at 38.1° in the plane of the membrane by five circle thin film XRD on Au nanorods.

further examined by WAXRD and five circle thin film XRD, as shown in figures 4(a)–(d). Gold nanorods obtained using 0.15 wt% solution and voltage of 2.0 V for 1 h show preferred orientation along the [111] direction. Curves in figures 4(a) and (b) show the powder diffraction patterns for AuNRs/AuNTs imbedded in a PC membrane, where the [111] and [222] peaks (2θ = 38.1° and 81.7°, respectively) of gold are observed (consistent with JCPDS 04-0784). The aligned AuNRs on Ti metal substrates after dissolving away the PC membrane also show preferred orientation along [111]. XRD patterns obtained from the free-standing AuNRs are consistent with those of the literature [11, 21, 22]. A step scan for 2θ = 36.1°–40.1° demonstrates that the [111] position (2θ = 38.1°) consists of many peaks at 2θ = 37.4°–38.6°, as shown in figure 4(c). I.e., the AuNRs are tilted and fulfil the Bragg's law from 2θ = 37.4° to 38.6°. To further clarify the orientation [111] of AuNRs to the normal direction of substrate, ω and ϕ scans are performed. The ω rocking from 0 to +10° with 2θ

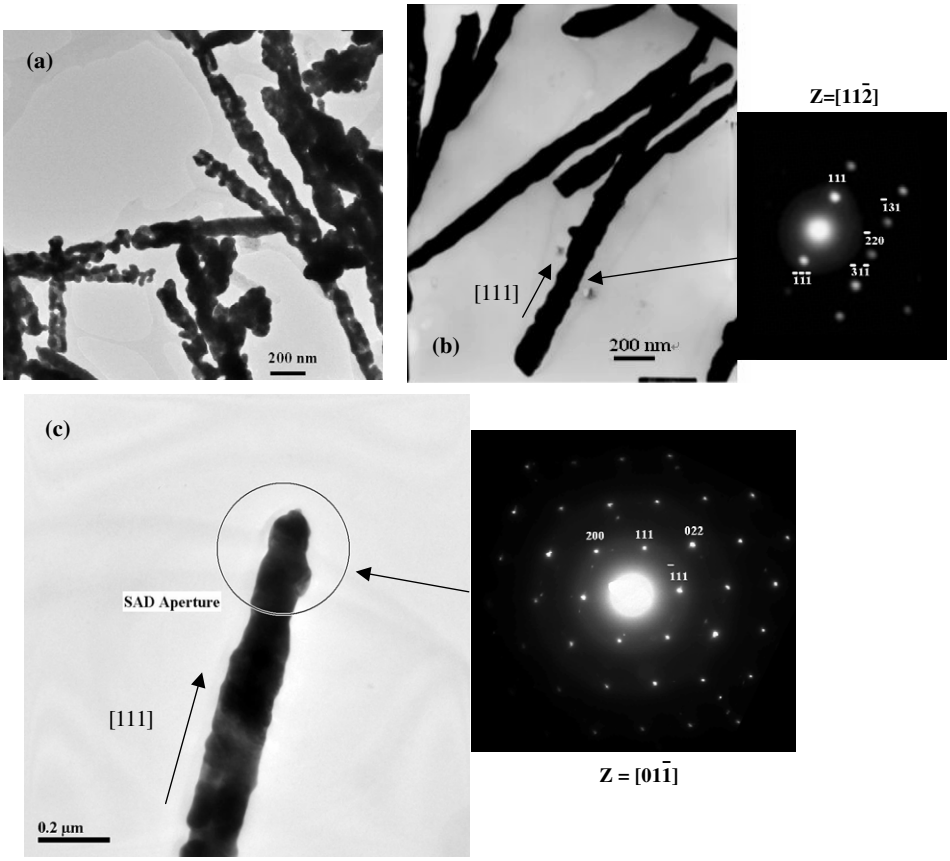

Figure 5. TEM micrograph for (a) porous gold nanorods obtained at voltage 5.0 V/1 h and (b), (c) bamboo-like free-standing Au nanorods obtained at 2.0 V/1 h for 0.15 wt% gold solution. Electron diffraction patterns for segments of single crystal taken from (b) zone axis at [11$\bar{2}$] and (c) zone axis at [01$\bar{1}$].

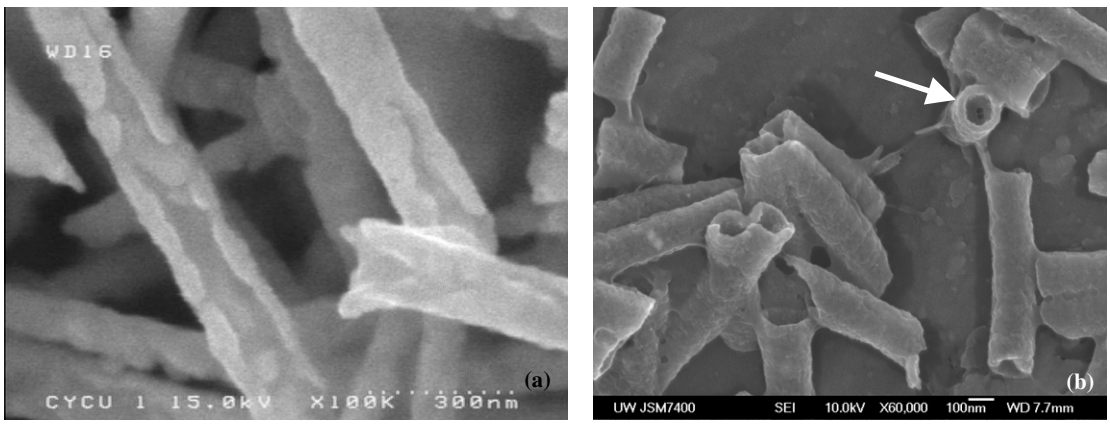

Figure 6. Incomplete nanotube obtained (a) at 0.05 wt% gold solution, applied voltage 1 V for 2 h, and (b) at 0.1 wt% gold solution, applied voltage 1 V for 1 h. The wall thickness of the nanotube around 30 nm is identified (white arrow).

fixed at 38.1° shows a broad and gradually declined intensity (not shown), indicating significant tilt of AuNRs from the vertical direction for more than 20°. This is attributed to the nature of the membrane used, where more than 10^8 pore channels per cm^2 can hardly be perfectly parallel. For the ϕ scan, the substrate spins and the *c* axis keeps stationary and perpendicular to the incident x-ray ($\psi = 90°$), i.e. *a* and *b* axes rotate through 360° about the *c* axis. The x-ray is incident in the plane of the membrane, which contains 10 μm long Au nanorods. The detector is fixed in the plane of the membrane at δ angle = 38.1°, where satisfactory Bragg's conditions can be detected. Four major broad peaks are observed for ϕ rotated from 0 to 360°, as shown in figure 4(d). Each broad peak corresponds to satisfactory Bragg's conditions for one axis in a half sphere (0–180°). The broadness of peaks indicates the significant tilt and polycrystalline nature of the synthesized

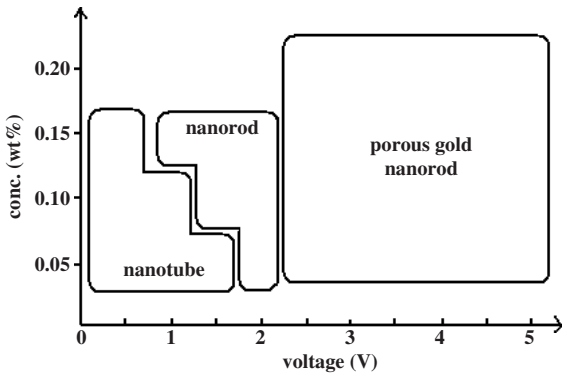

Figure 7. The formation map of gold nanotubes and nanorods at various concentrations and deposition voltages for 1 h duration.

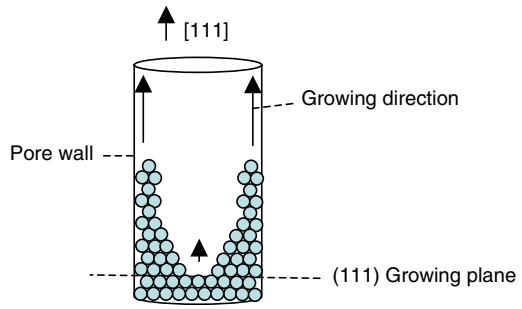

Figure 8. Growing mechanism from nanotubes into nanorods inside a 100 nm pore channel of the membrane. The growing speed on the pore wall is more rapid than that of the central part. Gold atoms are preferentially deposited on the (111) plane.

(This figure is in colour only in the electronic version)

AuNRs imbedded in the membrane. Further confirmation of crystal orientation of a single nanorod is accomplished by TEM observation.

Applied voltage at 5.0 V for electrochemical deposition results in porous and random-oriented polycrystalline gold nanorods as shown in figure 5(a). The high voltage causes water electrolysis and bubbles in the solution during deposition and thus results in porous morphologies. When deposition voltage reduces to 2.0 V, [111]-oriented gold nanorods result. A TEM micrograph shown in figure 5(b) demonstrates the typical nanorods obtained using 0.15 wt% and an applied voltage at 2.0 V for 1 h. These nanorods are slightly bumpy on their surface, but much more smooth and dense than those of 5.0 V. The growing direction is along [111], with two zone axes identified by moving a convergent electron beam along the longitudinal direction, as shown in figure 5(b) and the selected area diffraction (SAD) pattern in figure 5(c). This is consistent with the observation of Tian [10, 11] that the gold nanorods are actually in a bamboo-like structure when a medium voltage is used. The length of the single-crystalline segment increases when the potential is further reduced to 1 V. Figures 6(a) and (b) show the incomplete nanotubes obtained at 0.05 wt%, 1 V for 2 h and 0.1 wt%, 1 V for 1 h, respectively. This evidence suggests that at low concentration Au atoms reduce and deposit on the wall of the pore channel and gradually form nanotubes. A summary of the formation map deposition

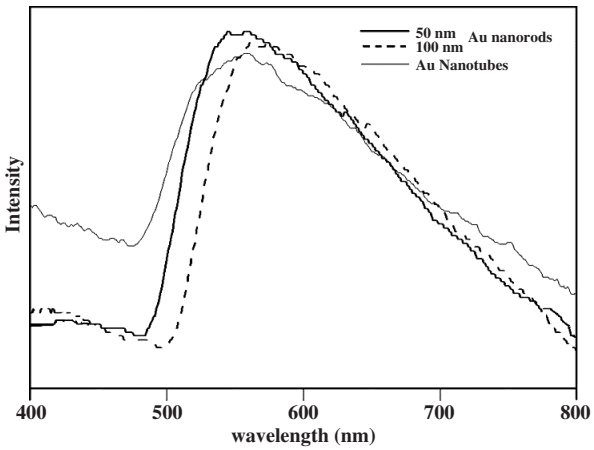

Figure 9. UV–visible absorption spectra for 50 and 100 nm gold nanorods and 100 nm nanotubes.

at various gold concentrations (0.05–0.2 wt%) and applied voltages (0.5–5 V) for 1 h duration is shown in figure 7. At low concentration ($\leqslant$0.1 wt%) and low deposition voltage ($\leqslant$1.0 V), nanotubes form predominantly. High voltage greater than 2.5 V usually results in polycrystalline and porous Au nanorods. For the template-growth experiments using 50 nm membranes, only [111] nanorods and no nanotubes are observed. In other words, formation of nanotubes and subsequent transformation to nanorods is only observed in the 100 nm pore size membrane.

Tian [10] proposed a 3D nucleation–coalescence growth mechanism for polycrystalline nanorods at high voltages, and a 2D nucleation and growing process for single crystals at low voltages. This reasonable growing mechanism is based on their 10 nm pore size template membranes. However, growing nanorods using 100 nm pore size membranes is slightly different from Tian's mechanism. In our study, nanotubes form first and progressively get thicker into nanorods in the 100 nm pore channels. Concentration of Au(III) solution, deposition voltage, and deposition duration are important factors in growing solid gold nanorods, since at low concentration nanotubes are always observed (figures 3(d) and 6(a), (b)), and at high concentration solid nanorods usually result. A growing mechanism proposed in figure 8 is thought to be responsible for the formation of nanotubes and subsequently solid nanorods. The wall of the pore channel in the PC membrane will be coated by gold initially due to heterogeneously faster depositing rate and finally grow into nanotubes. However, at long deposition duration (>5 h for 0.1 wt% Au solution), solid nanorods will be eventually formed by the lateral direction on the (111) plane toward the centre of the pore channel, i.e. starting with a tube, the wall of the tube gets progressively thicker and eventually sealed up to form nanorods. At concentration greater than 0.1 wt%, solid nanorods probably grow more homogeneously on the densest plane (111) and along the direction of [111] according the 2D mechanism proposed by Tian [10].

Figure 9 shows the UV–visible absorption spectra for gold nanorods and nanotubes. It is clear that 50 and 100 nm gold nanorods exhibit absorption peaks at 545 and 578 nm, respectively. The 100 nm nanotubes have

an absorption peak at 548 nm. The wall thickness of nanotubes is estimated to be 30 nm. Lower absorption peaks closer to the characteristic peak of gold nanoparticles (520 nm) seem to account for AuNRs and AuNTs with thinner diameter/thickness. Gold nanorods exhibit two absorption modes, which are the longitudinal mode and transverse mode [23–27]. The transverse (width) mode of the nanorods can be identified to be the absorption near 520 nm, which is essential in characterizing the optical properties of gold nanoparticles. For aspect ratio of gold nanorods over 3.0, another absorption maximum at 710 nm, which would also shift to near-IR regions at higher aspect ratios, corresponding to the absorption from the longitudinal mode, should be observed [23–29]. However, in our case, the longitudinal direction of the nanorods is 10 μm and the aspect ratio of AuNR/AuNT is high (50–100). No absorption peaks in UV–vis were observed. However, the longitudinal plasmon modes of the nanorods will contribute to the scattering response beyond the wavelength longer than ∼2000 nm based on the studies of nanorods with aspect ratios on the order of 20 [28, 29]. Hence the lack of absorption peak of the longitudinal mode is due to the limitation of the detection wavelength of the spectrometer we used.

4. Conclusion

Standing [111] crystalline gold nanorod and nanotube arrays synthesized using template growth and the electrochemical deposition method without organic additives has been presented. Unidirectional segments of single crystals and bamboo-like crystalline AuNRs, having diameter of 100–150 nm and a length of about 10 μm, are obtained. Absorptions in UV–visible spectra from transverse mode at wavelength 545 and 578 nm for 50 and 100 nm nanorods are observed, respectively. A growing mechanism complementary to the literature is suggested. Using a membrane with 100 nm pore size, gold nanotubes are initially formed from the bottom and the wall of the pore channels. Preferred growing on the pore walls at low gold concentrations and low voltages is proposed to be responsible for the formation of nanotubes which are progressively thicker and sealed up into nanorods at longer duration.

Acknowledgments

The financial support of this research by NSC 93-2113-M-033-006 and NSC 93-2745-M-033-004 is gratefully acknowledged. The assistance of TEM expert Dr Jong-Shing Bow and five circle thin film XRD expert Mr Shuh-Chin Lai is greatly appreciated.

References

[1] Tseng Y G and Ellenbogen J C 2001 *Science* **294** 1293
[2] Cao G Z 2004 *Nanostructures and Nanomaterials* (London: Imperial College Press)
[3] Masuda H and Fukuda K 1995 *Science* **268** 1466
[4] Martin C R 1994 *Science* **266** 1961
[5] Foss C A Jr, Hornyak G L, Stockert J A and Martin C R 1992 *J. Phys. Chem.* **96** 7497
[6] Martin C R 1996 *Chem. Mater.* **8** 1739
[7] Limmer S J and Cao G Z 2003 *Adv. Mater.* **15** 427
[8] Huber C A, Huber T E, Sadoqi M, Lubin J A, Manalis S and Prater C B 1994 *Science* **263** 800
[9] Zhao W B, Zhu J J and Chen H Y 2003 *J. Cryst. Growth* **258** 176
[10] Tian M L, Wang J G, Kurtz J, Mallouk T E and Chan M H W 2003 *Nano Lett.* **3** 919
[11] Wang J G, Tian M L, Mallouk T E and Chan M H W 2004 *J. Phys. Chem.* B **108** 841
[12] Gai P L and Harmer M A 2002 *Nano Lett.* **2** 771
[13] Gao T, Meng G W, Zhang J, Wang Y W, Liang C H, Fan J C and Zhang L D 2001 *Appl. Phys.* A **73** 251
[14] Molares M E T, Van Buschmann D D, Neumann R, Scholz R, Schuchert I U and Vetter J 2001 *Adv. Mater.* **13** 62
[15] Sauer G, Brehm G, Schneider S, Nielsch K, Wehrspohn R B, Choi J, Hofmeister H and Gosele U 2002 *J. Appl. Phys.* **91** 3243
[16] Barbic M, Mock J J, Smith D R and Schultz S 2002 *J. Appl. Phys.* **91** 9341
[17] Zhang J, Wang X, Peng X and Zhang L 2002 *Appl. Phys.* A **75** 485
[18] Chen J, Reed M A, Rawlett A M and Tour J M 1999 *Science* **286** 1550
[19] Reed M A, Chen J, Rawlett A M, Price D W and Tour J M 2001 *Appl. Phys. Lett.* **78** 3735
[20] Zhang X Y, Zhang L D, Lei Y, Zhao L X and Mao Y Q 2001 *J. Mater. Chem.* **11** 1732
[21] Zhao W B, Zhu J J and Chen H Y 2003 *J. Cryst. Growth* **258** 176
[22] Wang Z, Su Y K and Li H L 2002 *Appl. Phys.* A **74** 563
[23] Yu Y Y, Chang S S, Lee C L and Wang C R C 1997 *J. Phys. Chem.* B **101** 6661
[24] Chou C H, Chen C D and Wang C R C 2005 *J. Phys. Chem.* B **109** 11135
[25] West R, Wang Y and Goodson T III 2003 *J. Phys. Chem.* B **107** 3419
[26] Kwok S K and Ellenbogen J C 2002 *Mater. Today* **5** 28
[27] Joachim C, Gimzewski J K and Aviram A 2000 *Nature* **408** 541
[28] van der Zande B M I, Böhmer M R, Fokkink L G J and Schönenberger C 2000 *Langmuir* **16** 451
[29] Jana N R, Gearheart L and Murphy C J 2001 *J. Phys. Chem.* B **105** 4065